Available online at www.sciencedirect.com
ScienceDirect
International Journal of Hydrogen Energy 32 (2007) 1999–2004
International Journal of HYDROGEN ENERGY
www.elsevier.com/locate/ijhydene

Molecular dynamics study of hydrogen adsorption in carbonaceous microporous materials and the effect of oxygen functional groups

M. Georgakis*, G. Stavropoulos, G.P. Sakellaropoulos

Department of Chemical Engineering, Aristotle University, Thessaloniki, Greece

Received 20 July 2006; accepted 24 August 2006
Available online 18 October 2006

Abstract

This work attempts to shed light on molecular hydrogen adsorption in carbonaceous microporous materials by exploiting molecular dynamics simulations combined with geometry optimization calculations of the solid structures. Carbon structures were considered here because of evidence suggesting that they may be efficient media for hydrogen storage. The inclusion of oxygen functional groups in these solid structures was also examined since they could affect hydrogen adsorption. Insertion of oxygen functional groups causes a decrease in hydrogen adsorption and this effect is more evident in narrow pores. Hydrogen molecules adsorb in the pores as structured layers, depending on pore slit width. The amount of hydrogen adsorbed reached 4.41% w/w for the purely carbonaceous materials, whereas for the oxygenated materials adsorption was limited to 3.30% w/w. The estimated adsorption density inside the pores exceeded the liquid hydrogen density for both solid structures investigated.

Keywords: Molecular hydrogen; Adsorption; Simulation; Carbon; Structural modeling; Activated carbons; Hydrogen storage

1. Introduction

Hydrogen is currently attracting attention as a clean energy carrier, as a fuel in zero emission plants and electric cars, and as a substitute of fossil fuels. For most applications hydrogen storage is the greatest barrier to overcome for its efficient use. Storage should not be expensive and it should comply with international environmental and safety laws. US DOE has set a lower limit for storage at 6.5% w/w (extractable hydrogen).

Several methods have been proposed to date for hydrogen storage, such as liquefaction, compression, physisorption, chemisorption and metal hydride formation. Both liquefaction and compression suffer from high costs, while compressed hydrogen requires safe storage in heavy pressure vessels at extremely high pressures. The materials which have been examined for hydrogen adsorption (physisorption and chemisorption) are mostly carbonaceous. These materials are usually of graphitic nature and consist either of slit like pores or of carbon nanotubes [1] because of their special structural properties.

Considerable controversy exists regarding the adsorptive capacity of nanotubes and graphitic carbons, and the effect of intercalated atoms (such as potassium or oxygen) on hydrogen adsorption. Dillon et al. [2] reported promising hydrogen adsorption (5–10% w/w) on single wall carbon nanotubes (SWNT), causing a turn in scientific research towards SWNTs. Liu et al. [3] reported a 4–5% w/w of hydrogen adsorption on SWNTs, at 100 atm and room temperature, while Ye et al. [4]measured a H/C ratio of about 1/1 for hydrogen on SWNT at 80 K. Recent results for hydrogen adsorption on multi wall carbon nanotubes (MWNTs) give 1.97% w/w (40 bar) [5], 3.7% w/w (69 bar) [6], 4% w/w (100 bar) [7] and 6.3% w/w (148 bar) [8]. Tibbetts and Meisner [9] and Shiraishi et al. [10] suggested that any claim for adsorption higher than 1% by weight is due to experimental errors and they reported a capacity of 0.3% by weight.

Chen et al. [11] reported that by doping carbon nanotubes with lithium and potassium hydrogen adsorption reached 14–20% by weight between 400 °C and room temperature. They proposed that a chemical dissociation takes place inside

* Corresponding author. Tel.: +30 2310 996260; fax: +30 2310 996168.
E-mail address: mgeorgak@eng.auth.gr (M. Georgakis).

0360-3199/$ - see front matter © 2006 International Association for Hydrogen Energy. Published by Elsevier Ltd. All rights reserved.
doi:10.1016/j.ijhydene.2006.08.040

the nanotubes. This report was followed by a number of experimental studies [12–20], which led to controversial results, as discussed by Ding et al. [19]. Intercalation of potassium in graphitic nanofibers is suggested to increase hydrogen storage up to a factor of ten [20], attributed to widening of the pores [21]. Froudakis [22,23] studied this phenomenon using advanced simulation methods. He suggested that increased hydrogen adsorption was due to a charge transfer from K atoms to the nanotube and a subsequent polarization of the hydrogen molecules by the positively charged K atoms.

Several theoretical studies [24–34] of hydrogen adsorption on carbon nanotubes showed that the DOE-proposed limit of 6.5% by weight could not be achieved. In the past 15–20 years, many efforts have been made to prepare active carbons with increased hydrogen storage capacity. A recent review [35] indicates that microporous carbons are the only materials, which could reach the DOE goal of 6.5% w/w of extractable hydrogen. Most experimental studies show that a maximum capacity of about 2.5% w/w at low pressures (1–10 atm) [36,37], and 5.5% w/w at high pressures (up to 60 atm) [38,39] could be achieved. Thermodynamic studies, however, give conflicting results, with an adsorption of 0.03–1.90% w/w for a stack of graphitic sheets [40] or 0.05–2.25% w/w for isolated sheets [40] and 23.764% w/w as a maximum adsorption limit [41] at high pressures (80 MPa).

Modification of activated carbon could increase the adsorption of some gases [42]. The carbon surface can be modified by oxidation with oxygen, nitric acid or other oxidants to form oxygen containing functional groups. Early studies with activated carbons modified by gas phase oxidation indicated an increase in hydrogen adsorption at 400–700 °C [43]. However, oxidation of activated carbons by $(NH_4)_2S_2O_8$, caused a decrease in hydrogen adsorption [44].

The amount of hydrogen retained in carbon structures depends on the arrangement of hydrogen molecules in the pores, which can result in adsorbed phase densities higher than those of the liquid. Theoretical studies [45–54] on microporous carbons suggest that sorption leads to adsorption densities greater than the respective liquid densities of the gases used [46,51,55–58]. Gadiou et al. [59] prepared ordered microporous carbonaceous solids and measured hydrogen densities up to 0.1 g cm^{-3}, which is definitely higher than the liquid hydrogen density (0.071 g cm^{-3}). Increase of density in the pores is a key factor in adsorption calculations and it was a subject of investigation in the present work.

Apparently, recent theoretical and experimental studies do yield ambiguous conclusions for the adsorption of hydrogen on the materials studied. This paper aims at evaluating theoretically the maximum adsorption capacity for hydrogen on microporous carbonaceous materials, and if the DOE-proposed limit of 6.5% w/w of extractable hydrogen can be achieved. In addition, the effect of oxygen insertion into the solid structures was examined with regard to hydrogen adsorption, employing the same technique. For these evaluations, solid models were constructed and used for molecular dynamics simulations of hydrogen adsorption on slit shaped micropores of carbonaceous materials.

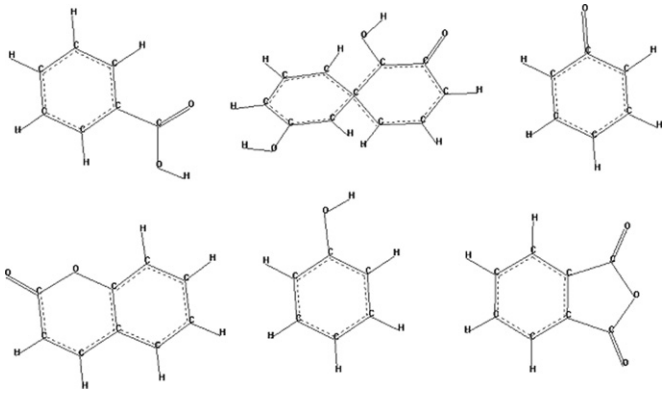

Fig. 1. The six oxygen functional groups used in this study.

2. Structural modeling and simulations

In order to simulate the solid structure of microporous active carbons, structure modeling has been used. The first model accounts for the purely carbonaceous material, whereas the second model depicts the solid structure after insertion of oxygen in the form of various functional groups.

The basic (non-oxygenated) structure comprises benzene rings placed side by side, forming a planar sheet of dimensions 20×25 Å (approximately). Geometry optimization calculations were employed to obtain the final structure of every sheet. Six single sheets placed in parallel were used to form a slit shaped pore model. The distance between the carbonaceous sheets was set to 3.4 Å in accordance with the graphitic structure. Several slit pore diameters were examined, ranging from 5 to 20 Å.

For the second model described, various oxygen functional groups were inserted into the previously described single sheet model. Six typical oxygenated structures were employed, Fig. 1, which are typically encountered in active carbons. Additional geometry calculations were performed which resulted in graphene sheets that were no longer flat, as shown in Fig. 2. The oxygen content was set at 3% w/w, which is a typical value for such carbons. The slit pore diameters used with this model were the same as the ones of the purely carbonaceous structure.

Hydrogen was considered to be in molecular form. It was used in "clouds" of 200–500 hydrogen molecules, which were first allowed to equilibrate at the simulation temperature of 77 K. The latter is the typical temperature of experimental hydrogen adsorption tests.

Hydrogen adsorption on the two structures described above (purely carbonaceous material, and oxygenated material) was examined by molecular dynamics simulations. The time step was set at 10^{-15}–10^{-16} s and the total simulation time exceeded 300 ps per simulation. If shorter time steps were used, the system could not reach adsorption equilibrium due to the shorter vibration times of the hydrogen–hydrogen bond. If shorter time steps were used, the simulation time would exceed acceptable limits.

All simulations were performed using multiple licenses of the HyperChem 7.5, HyperCube, USA software. We needed up

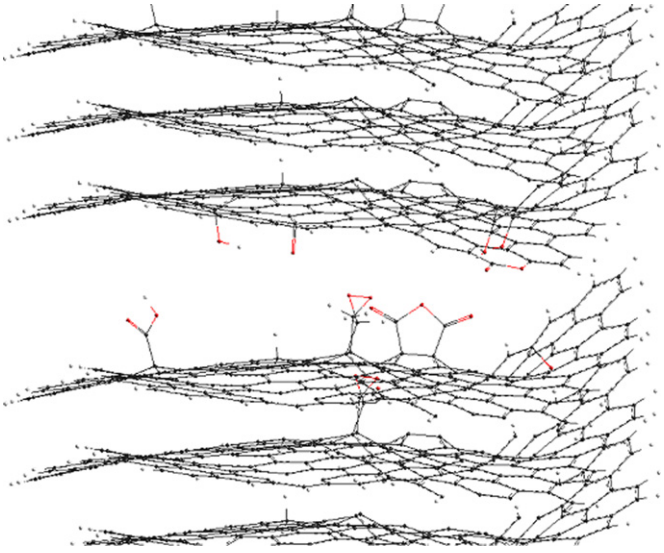

Fig. 2. The oxygenated slit shaped model derived in this study.

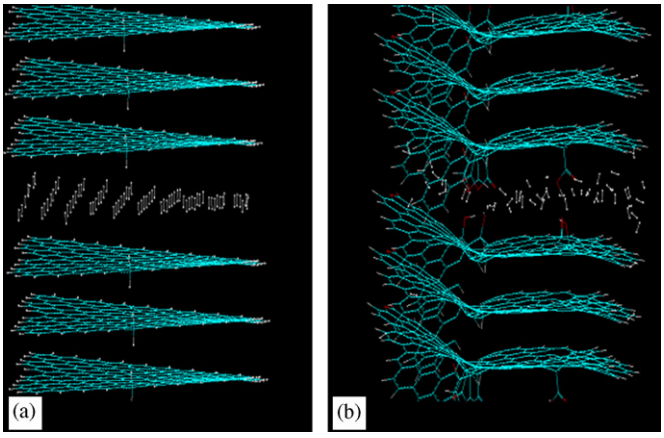

Fig. 3. Hydrogen adsorption snapshots for the pore size of 7 Å: (a) purely carbonaceous material; (b) oxygenated materials, at simulation times of 240 ps, when the adsorption simulation is complete in the basic model solid.

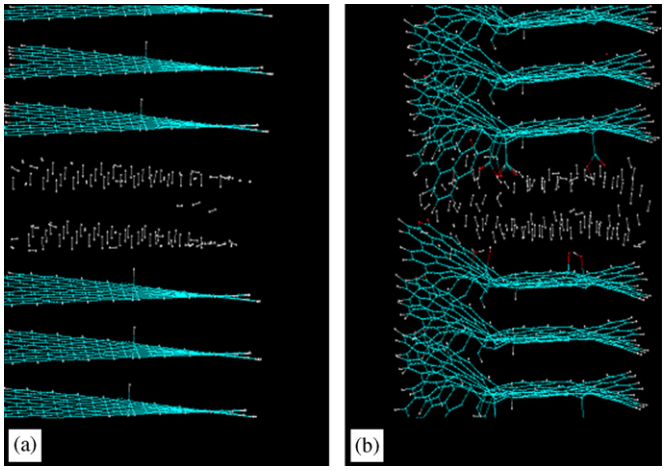

Fig. 4. Hydrogen adsorption snapshots for the pore size of 10 Å: (a) purely carbonaceous material; (b) oxygenated materials, at simulation times of 350 ps, when the adsorption simulation is complete in the basic model solid.

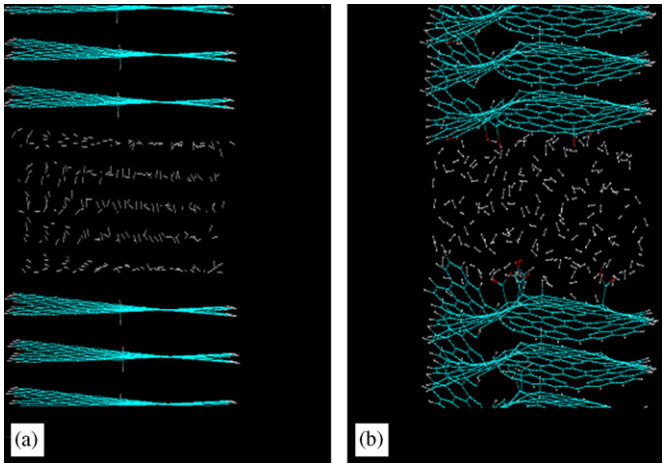

Fig. 5. Hydrogen adsorption snapshots for the pore size of 15 Å: (a) purely carbonaceous material; (b) oxygenated materials, at simulation times of 560 ps, when the adsorption simulation is complete in the basic model solid.

to 5 licenses in order to complete our study within acceptable time limits.

3. Results and discussion

The solid structures derived by geometry optimization simulations give planar layers of hexagonal benzene rings as shown in Figs. 3–5. These planes (Figs. 3a, 4a, 5a) are not flat, as in the case of graphitic layers, but slightly distorted. Plane distortion is more pronounced in the presence of oxygenated functional groups (Figs. 3b, 4b, 5b), which can also result to some bonding between the layers. The "view angle" of these structures is not the same in all figures; it was changed slightly in order to obtain a better insight of the pores' interior during adsorption. The number of hydrogen molecules required to completely fill each pore size varied from 80 for the 5.5 Å pores to 560 for the 20 Å pores (for the basic material).

Molecular dynamics simulations on the above models provide "snapshots" of molecular hydrogen adsorption in the slit pores. Simulations between 5 and 7 Å pores revealed that H_2 molecules enter the pores larger than 5.5 ± 0.1 Å. Figs. 3–5 show such snapshots for slit pore sizes of 7, 10 and 15 Å, for the basic structure and for the oxygenated solid structure.

Snapshots can be obtained at any time in the course of hydrogen adsorption. The snapshots presented in Figs. 3–5 are the final ones, after all hydrogen molecules have entered and been adsorbed in each pore slit. This time is not the same for all pore sizes and varies from 150 ps for 5.5 Å pores to 240, 350, 560 and 900 ps for the 7, 10, 15 and 20 Å pores, respectively. Somewhat larger computational times (by 15–20%) were necessary for full hydrogen entrance and organization in oxygenated pores. For comparison, Fig. 6 gives an enlarged view of a 10 Å pore at 270 ps of adsorption, i.e. before the end of the adsorption process.

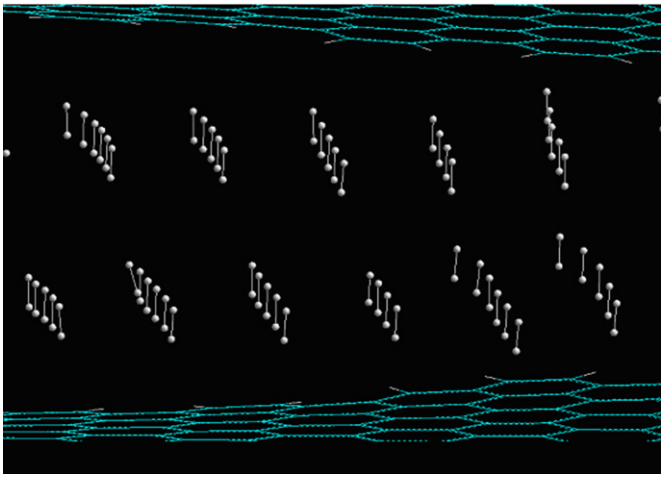

Fig. 6. A magnified snapshot of the adsorption process in the 10 Å pores of the pure materials at simulation time of 270 ps.

Table 1
Minimum C–H distance in the pore sizes used for the purely carbonaceous material (A-series)

Pore size (Å)	5.5	7	10	15	20
Minimum C–H distance (Å)	2.750	2.811	2.835	2.851	2.892

All figures show that, upon entering the pores, hydrogen molecules are organized in layers parallel to the solid planes, following the planes' distortion. In 5.5 Å pores, H_2 molecules orient themselves parallel to the slit walls, while in larger pores they align in groups and orient themselves perpendicular to the wall surface. The number of hydrogen molecules in each group varies with adsorption time; for example, in 10 Å pores, hydrogen groups consist of 4–6 molecules at 270 ps (Fig. 6), and of 8 molecules, at distances of 2.80–2.85 Å at the end of the simulation process (350 ps). Comparison of Figs. 3a–5a with 3b–5b reveals that for the same slit size and adsorption time the layers have similar but not identical structure. The oxygenated groups on the surface seem to delay the layer formation and organization, thus resulting in slower hydrogen adsorption.

Entrance of hydrogen molecules into the pores and their organization in groups and layers depends not only on the slit width but also on the Van der Waals (VdW) radii of carbon (1.7 Å) and hydrogen (1.2 Å) atoms. Based on these VdW radii, the smallest pores for which H_2 penetration would take place (with H–H molecules parallel to the walls), should be 5.8 Å ($2 \times 1.7 + 1.2$). This is in agreement with the size of 5.5 Å reported above as the minimum pore width for H_2 adsorption. The difference of 0.3 Å represents a decrease in the C–H distance by 5.1%. In larger pores, this decrease is smaller (2.21% for 7 Å pores, 0.7% for 10 Å pores). This decrease in the VdW radii is attributed to the increased need for optimum arrangement of molecules in the narrow pores where the available space is limited and to the physical adsorption forces (dispersion forces). Table 1 summarizes the minimum C–H distances observed for various pore sizes of the basic structure used.

Table 2
Number of layers formed at each pore size

Pore Size (Å)/solid model	5	5.5	7	10	15	20
Pure material	0	1	1	2	5	6
Oxygenated material	0	1	1	2	4	6

Table 3
Estimation of critical pore sizes for layer formation (±0.2 Å)

Number of layers	1	2	3	4	5	6
Pore size (Å)	5.5	7.8	10.2	12.5	14.8	17.1

Depending on the slit width more than one hydrogen layer can be formed, as shown in Figs. 3–6. Table 2 gives the number of hydrogen layers formed in the various pore widths examined, while Table 3 shows the estimated critical pore dimensions for the transition from one to two and up to six layers of adsorbed hydrogen molecules. These estimates are important for the "design" of microporous materials for optimum hydrogen physical adsorption. They also allow interpretation of variations in adsorption densities, as discussed later.

Multilayer adsorption is expected to increase the amount of hydrogen adsorbed in the pores. Table 4 gives the calculated amount of hydrogen adsorbed per solid weight after optimum configuration of the gas molecules was attained. Results show a gradual increase of retained hydrogen with increasing pore dimensions. In all cases, however, the adsorbed amount is significantly lower for the oxygenated solid structures than for the purely carbonaceous ones. This is in agreement with available experimental data [60,61] and with the distortion of the structural planes caused by the oxygenated groups, as discussed before (see Figs. 3b–5b). Plane distortion and protruding oxygenated groups result in steric hindrances, and in less available space for the hydrogen molecules to organize in layers. In addition, the insertion of oxygen groups into the solid causes an increase of the solid's weight by 5.81%, which would also decrease somewhat the adsorbed amount per solid weight. Finally, oxygen–hydrogen interactions are weaker than the carbon–hydrogen ones at this adsorption temperature. The latter could by validated only by ab initio or DFT calculations. In any case, the observed decline of H_2 adsorption in oxygenated structures cannot be explained by the volume occupied by the oxygenated structures, which is very low (101 ± 5 Å^3), compared to the total pore volume (e.g. 2750 Å^3 for the 5.5 Å pores, and 10, 000 Å^3 for the 10 Å pores).

From the adsorbed amount and the pore volume in each case, the adsorption densities can be estimated, Table 4. In all pores, the adsorption density was found to be significantly higher than the liquid hydrogen density, which is 0.071 g cm^{-3}. This implies that the adsorbed molecules are already in a compressed state, and greater driving forces are needed in order to attain a better configuration. Such an extra driving force could be the presence of structural imperfections in the solid, which is currently under investigation.

Compression of gases (H_2 and N_2) inside various solid materials has been reported by several investigators [38,35,46–50].

Table 4
w/w % adsorption (%g g^{-1}), adsorption density inside the pores (g cm^{-3}), and adsorption density based on the solid volume (g cm^{-3}) for both model solids used in this study

Pore sizes (Å)	w/w% adsorption		Adsorption density (g cm^{-3})		Adsorption density on solid volume (g cm^{-3})	
	Basic model	Oxygenated model	Basic model	Oxygenated model	Basic model	Oxygenated model
5.5	0.67	0.21	0.065	0.020	0.0188	0.0056
7	1.56	0.58	0.106	0.045	0.0364	0.0149
10	2.18	1.55	0.103	0.084	0.0444	0.0349
15	3.52	2.40	0.112	0.086	0.0592	0.0447
20	4.41	3.30	0.105	0.088	0.0630	0.0522

The techniques used in those studies are mostly stochastic ones (GCCM). In the present work, this phenomenon is observed via molecular dynamics simulations. To the best of our knowledge, this is the first time that MD has been utilized for this purpose.

The adsorption density (adsorbed amount per free volume) is always higher for the pure materials. The difference is as high as 57% for small pores (7 Å), probably caused by steric hindrance effects by the oxygen functional groups. The volume of such narrow pores is already hard to access; therefore, the addition of extra barriers such as oxygen groups hinders adsorption. On the other hand, the case for the larger pores is different. In the larger pores, the difference ranges from 16% to 23.5%, strengthening the hypothesis of the steric hindrance effects caused by the narrower pores.

For all pore sizes examined, the adsorbed amount of hydrogen is below the DOE target of 6.5% w/w of extractable hydrogen (Table 4). The maximum amount adsorbed was found to be 4.41% w/w for the purely carbonaceous materials and 3.30% w/w for the oxygenated structures in the 20 Å pores. This result is in agreement with previous theoretical studies of hydrogen adsorption in such materials [40] and with experimental studies [36,37], which typically yield an adsorbed amount of 2.5% w/w at low pressures (1–10 atm). The estimated value gives the ideal amount adsorbed, which is likely to be higher than the experimental one. Pore blocking, among others, hinders access to some micropores of real carbonaceous materials, thus, decreasing the adsorbed amount. One could assume that the use of a "lighter" pore model, comprising less than three parallel sheets per wall, would lead to a higher % w/w hydrogen adsorption. The model constructed here is generally accepted as representative of the nature of activated carbons. Of course, in real activated carbon lighter pore structures also exist, having one or two parallel sheets, and such structures merit further investigation.

The results of Table 4 on adsorbed H_2 density show an "abnormal" variation with increasing pore size (cf. densities for pores of 7–10 and 15–20 Å). To explain this behavior, one should resort to the number of H_2 layers formed in each pore size (Table 1) and to the critical pore widths at which an additional H_2 layer is formed. Table 3 shows the slit widths at which these transitions occur. Among the chosen pore sizes for simulations (5.5, 7, 10, 15, 20 Å) some are closer to these critical widths than others. For example, the calculated adsorption in the 7 Å pore is higher than that in the 10 Å pores because the 7 Å size is closer to the critical width of the first layer formation than the 10 Å size is to the critical width of the second layer formation. The 10 Å pores contain two H_2 layers (Table 1) based on the simulations, while they are very close to the transition width at which a third layer is formed (10.3 Å, Table 3). Therefore, the H_2 adsorption density is lower in the 10 Å pores than in the 7 Å ones. Similar considerations apply for the 15 and 20 Å pores.

These estimations are valid for the pure material studied in this work. For the oxygenated structures the critical widths at which additional H_2 layers would be formed have not been estimated here. However, they are not expected to be significantly different from those for the pure material, based on the simulated snapshots, Figs. 3–5. In this case, steric effects caused by the oxygenated groups in the free pore volume should also be taken under consideration in adsorption density, as discussed before.

4. Conclusions

The presented work offers insight to the mechanism of physical adsorption of molecular hydrogen on carbonaceous materials. Two different model structures have been used combined with MD simulations in order to examine the microscopic characteristics of the adsorption process. The first model comprised only carbon and hydrogen atoms in the shape of hexagonal benzene rings, while in the second model six oxygen functional groups were also inserted.

For both models, hydrogen molecules enter pores larger than 5.5 Å. In the narrowest pores, hydrogen molecules orient themselves with their axis parallel to the solid walls, whereas in pores larger than 7 Å, they arranged in groups of up to 10 molecules, with their axis perpendicular to the pore walls.

Adsorption progresses with the formation of multiple layers of adsorbed molecules at exact pores sizes. In the layer formation process, the hydrogen–hydrogen distance gradually increases with pore size increase, mainly due to the growth of the available space inside the pores. Adsorbed hydrogen molecules are in a compressed state inside the solid pores, and the hydrogen density is higher than the liquid hydrogen density, which is 0.071 g cm^{-3}.

Hydrogen adsorption is always higher in the pure materials than in the oxygenated structures, due to three factors: steric hindrance effects, increase of solid weight for oxygenated

model, and weaker oxygen–hydrogen interactions compared to carbon–hydrogen ones. The greatest adsorption achieved was 4.41% w/w for the pure materials and only 3.30% w/w for the oxygenated ones, both for 20 Å pores.

The work presented here is important in hydrogen storage technology, in order to tailor-make materials of desirable physical properties. It indicates the optimum pore sizes which a carbonaceous material should posses in order to maximize hydrogen adsorption. Physisorption attractive forces alone cannot lead to a more efficient configuration of hydrogen molecules inside the pores. In order to enhance the adsorption process, physisorption forces should be augmented, for example by alteration of the solid structures via insertion of structural imperfections or of other elements.

References

[1] Iijima S. Nature 1991;354:56.
[2] Dillon AC, Jones KM, Bekkedahl TA, Kiang CH, Bethune DS, Heben MJ. Nature 1997;386:377.
[3] Liu C, Fan YY, Liu M, Cong HT, Cheng HM, Dresselhaus MS. Science 1999;286:1127.
[4] Ye Y, Ahn CC, Witham C, Fultz B, Liu J, Rinzler G. et al. Appl Phys Lett 1999;74:2307.
[5] Lee H, Kang Y-S, Kim S-H, Lee J-Y. Appl Phys Lett 2002;80:577.
[6] Lueking A, Yang RT. AIChE J 2003;49:1556.
[7] Li X, Zhu H, Ci L, Xu C, Mao Z, Wei B, Liang J, Wu D. Carbon 2002;39:2077.
[8] Hou P-X, Yang Q-H, Bai S, Xu S-T, Liu M, Cheng H-M. J Phys Chem B 2002;106:963.
[9] Tibbetts GG, Meisner CP, Olk CH. Carbon 2002;39:2291.
[10] Shiraishi M, Takenobu T, Ata M. Chem Phys Lett 2003;367:633.
[11] Chen P, Wu X, Lin J, Tan KL. Science 1999;285:91.
[12] Kelly KF. et al. Chem Phys Lett 1999;313:445.
[13] Yang RT. Carbon 2000;38:623.
[14] Zhu HWJ. Mater Sci Lett 2000;19:1237.
[15] Kuznetsova A, Mawhinney DB, Naumenko V, Yates Jr. JT, Liu J, Smalley RE. Chem Phys Lett 2000;321:292.
[16] Brown CM. et al. Chem Phys Lett 2000;329:311.
[17] Hirscher M. et al. Appl Phys A 2001;72:129.
[18] Cao A. et al. Chem Phys Lett 2001;342:510.
[19] Ding RG, Lu GQ, Yan ZF, Wilson MA. J Nanosci Nanotechnol 2001;1:7.
[20] Nijkamp MG. Inorganic chemistry and catalysis, PhD thesis. Debye Institute, Utrecht University, P.O. Box 80083, 3508 TB Utrecht, The Netherlands, 2002.
[21] Schimmel HG, Nijkamp G, Kearly GJ, Rivera A, de Jong KP, Mulder FM. Mater Sci Eng B 2004;108:124.
[22] Froudakis GE. Nano Lett 2001;1(10):531.
[23] Froudakis GE. Nano Lett 2001;1(4):179.
[24] Wang K, Johnson JK. Mol Phys 1998;95:299.
[25] Wang K, Johnson JK. J Chem Phys 1999;110:577.
[26] Wang K, Johnson JK. J Phys Chem B 1999;103:277.
[27] Wang K, Johnson JK. J Phys Chem B 1999;103:4809.
[28] Simonyan VV, Diep P, Johnson JK. J Chem Phys 1999;111:9778.
[29] Darkrim F, Levesque D. J Chem Phys 1998;109:4981.
[30] Rzepka M, Lamp P, de la Casa-Lillo MA. J Phys Chem B 1998;102:10894.
[31] Gordon PA, Saeger RB. Ind Eng Chem Res 1999;38:4647.
[32] Yin Y, McEnaney B, Mays T. Langmuir 2000;16:10521.
[33] Chen HS, Pez G, Kern G, Kress G, Hafner J. J Phys Chem B 2001;105:736.
[34] Claye AS, Fischer JE. Electrochem Acta 1999;45:107.
[35] Zhou L. Renewable Sustainable Energy Rev 2005;9(4):395–408.
[36] Parra JB, Ania CO, Arenillas A, Rubiera F, Palacios JM, Pis JJ. J Alloys Comp 2004;379:280–9.
[37] Chen GX, Hong MH, Ong TS, Lam HM, Chen WZ, Elim HI. Carbon 2004;42:2735–77.
[38] Panella B, Hirscher M, Roth S. Carbon 2005;43:2209–14.
[39] Dillon AC, Heben MJ. Appl Phys A 2001;72:133–42.
[40] Touzik A, Hermann H. Chem Phys Lett 2005;416:137–41.
[41] Zhang L, Li K, Zhu X, Lv C, Ling L. Letters to the editor. Carbon 2002;40:445–67.
[42] Bansal RC, Donet J-P, Stoeckli F. Active carbon. New York: Marcel Dekker; 1988.
[43] Agarwal RK, Noh JS, SchwarzP JA. Davini. Carbon 1987;25: 219–26.
[44] Takagi H, Hatori H, Yamada Y, Matsuo S, Shiraishi M. J Alloys Compds 2004;385:257–63.
[45] Dobruskin VKh. Carbon 2002;40:659.
[46] Suzuki T, Kaneko K, Setoyama N, Maddox M, Gubbins K. Carbon 1996;34:909.
[47] Yins YF, McEnaney B, Mays TJ. Carbon 1998;36(10):1425.
[48] Okayama T, Yoneya J, Nitta T. Fluid Phase Equilibria 1995;104:305.
[49] Jagiello J, Thommes M. Carbon 2004;42:1227.
[50] Do DD, Do HD. Langmuir 2004;20:7103.
[51] Challet S, Azais P, Pellenq RJ-M, Isnard O, Soubeyroux J-L, Duclaux L. J Phys Chem Solids 2004;65:541.
[52] Bhatia SK, Tran K, Nguyen TX, Nicholson D. Langmuir 2004;20:9612.
[53] Biggs MJ, Buts A, Williamson D. Langmuir 2004;20:5786.
[54] Jeloaica L, Sidis V. Chem Phys Lett 1999;300:157.
[55] Breck DW, Grose RW. In: Meier WM, Uytterhoeven JB, editors, Molecular sieves, vol. 319. Washington, DC: American Chemical Society; 1973.
[56] Goulay AM, Tsakiris J, Cohen de Lara E. Langmuir 1996;12:371.
[57] Klein J, Kumacheva E. Science 1995;269:816.
[58] Carrott PJM, Roberts RA, Sing KSW. A new method for the determination of micropore size distribution. In: Unger KK, Rouquerol J, Sing KSW, Kral H, editors, Characterization of porous solids, vol. 89. Amsterdam, The Netherlands: Elsevier; 1988.
[59] Gadiou R, Saadallah S-E, Piquero T, David P, Parmentier J, Vix-Guterl C. Microporous Mesoporous Mater 2005;79:121–8.
[60] Takagi H, Hatori H, Yamada Y, Matsuo S, Shiraishi M. J Alloys Compds 2004;385:257–63.
[61] Agarwal RK, Noh JS, Schwarz JA, Davini P. Carbon 1987;25(2): 219–26.